Sustainable Energy & Fuels

ROYAL SOCIETY OF CHEMISTRY

PAPER

View Article Online
View Journal | View Issue

Cite this: *Sustainable Energy Fuels*, 2024, **8**, 4956

Simple and sustainable electric power generation by free evaporation of liquids from the surface of a conventional thermoelectric generator†

Pengfei Cheng, * Dong Wang * and Peter Schaaf

Liquid evaporation, or water vapor generation, is a spontaneous natural process and is always accompanied by evaporation cooling. However, evaporation cooling that can directly produce electricity based on the Seebeck effect and even supply power for electronic devices has not yet been reported. Here, liquid evaporation generators (LEGs), with cheap and practical thermoelectric generators (TEGs), are demonstrated to generate electric power based on the combination of the Seebeck effect and evaporation cooling. We systematically explored the LEG based on water evaporation (w-LEG) in a real environment, and five tandem w-LEGs can produce a maximum voltage of 4.4 V and achieve a maximum power density of 5.4 mW cm^{-2}, which can successfully supply power for common electronic devices. Our concepts demonstrate a new supplement of green energy technology and a new direction for the applications of low temperature thermoelectric conversion (below 50 °C).

Received 21st August 2024
Accepted 15th September 2024

DOI: 10.1039/d4se01156b

rsc.li/sustainable-energy

Introduction

Approximately 500 000 km^3 of water evaporates from the surfaces of global oceans and continents annually,[1–3] which not only plays a crucial role in the earth's water cycle but also implies a huge heat exchange (approximately 1.2 × 10^{18} J per year).[2–4] Utilization of the heat exchange of the water evaporation for the conversion of electrical energy can become very interesting for sustainable development. For instance, some water evaporation-induced electricity devices based on the hydrovoltaic effect have attracted tremendous interest from researchers,[5–11] and the hydrovoltaic generator (HVG) can produce electricity from charge transfer at the solid–liquid interfaces.[11] But these devices face a lot of challenges, such as high cost, complex preparation, problems in large-scale production, low output voltage and low output power density, limiting their practical applications. To overcome the obstacles, new generator devices that take advantage of water evaporation and produce cost-effective output power are urgent to be developed. Herein, we propose a new strategy for power generation induced by evaporation, namely by free evaporation of liquids from the surface of a conventional thermoelectric generator (TEG). The power generation is based on the upper surface temperature of the thermoelectric device decreased by the evaporation of the liquid, leading to a temperature difference between both sides. Here we call it a liquid evaporation generator (LEG).

The TEG working principle is based on the Seebeck effect, also called the thermoelectric (TE) effect, by which electricity is generated when temperature differences (ΔT) exist in thermoelectric materials,[12,13] such as Bi_2Te_3[14,15] and SnSe.[16,17] The thermoelectric performance is evaluated using the figure of merit $ZT = S^2\sigma T/\kappa$, where S, σ, T and κ are the Seebeck coefficient, electrical conductivity, absolute temperature and thermal conductivity, respectively.[14] The open-circuit voltage (V_{OC}) produced by a thermoelectric generator is estimated from the formula:

$$V_{OC} = n \times (S_p - S_n) \times \Delta T$$

where n, S_p, S_n and ΔT stand for the number of the pairs of thermoelectric elements, Seebeck coefficients of p-type and n-type thermoelectric materials, and ΔT between the hot side and cold side of thermoelectric elements, respectively.[18] Normally, liquid spontaneous evaporation, such as water, ethanol, and acetone evaporation, needs to continuously absorb heat from bulk liquid and the ambient atmosphere, thus leading to a lower temperature on the surface of liquid than that of the ambient atmosphere, as known as evaporative cooling. So, ΔT between the liquid surface and the ambient atmosphere can be efficiently applied to generate electricity based on the Seebeck effect. As far as we know, however, LEGs based on the Seebeck effect have not been reported yet.

In addition, commercially available large-area TEGs are cheaper devices with easier fabrication than hydrovoltaic

Chair Materials for Electrical Engineering and Electronics, Institute of Materials Science and Engineering and Institute of Micro and Nanotechnologies MacroNano, TU Ilmenau, Gustav-Kirchhoff-Str. 5, 98693 Ilmenau, Germany. E-mail: pengfei.cheng@tu-ilmenau.de; dong.wang@tu-ilmenau.de

† Electronic supplementary information (ESI) available: Supplementary Fig. S1–S5, and Supplementary Video S1. See DOI: https://doi.org/10.1039/d4se01156b

systems, which involve complex fabrication processes and require expensive raw materials. Therefore, integrating high-efficiency, low-cost, and scalable TEGs with water evaporation cooling for electricity production can be a promising strategy to take advantage of the wasted evaporation energy for addressing the energy crisis.[19] Very important, water vapor can return to the earth by the atmospheric water cycle without any pollution,[20] and it can be reused for sustainable electricity generation.

Here, this new strategy is demonstrated by three types of LEGs which are clearly superior to the evaporation-induced generators based on the hydrovoltaic effect, including the LEGs with water, ethanol and acetone evaporation (they are denoted as the w-LEG, e-LEG, and a-LEG, respectively). For example, the w-LEG can produce comparable output voltage performance, with a much larger current density (over three orders of magnitude) compared to hydrovoltaic generators. The temperature change induced by liquid evaporation can be influenced by wind flow, and the performance of the w-LEG at different wind velocities in a low temperature environment, which is close to the practical conditions, has been systematically studied. To demonstrate the possibility of practical application, five w-LEGs are connected in series to exhibit a voltage of 4.4 V, which is larger than the two junctions of a commercial AA battery. They are also able to achieve a maximum power density of 5.4 mW cm^{-2}, which is much higher than that of recently reported water evaporation generators, while we used a much easier method and simpler experimental set-up. Furthermore, water is widely available and TEG modules are commercially available, thus the production of the w-LEG for generating electricity is easily scalable. The generation of electricity only needs liquid water, while the water vapor can return to the ground within the earth's water cycle. It represents a green way to generate electricity that can effectively reduce CO_2 emissions and relieve pressure on energy supply. We believe our findings open a new field for electric power generation based on the combination of evaporation cooling and the Seebeck effect.

Results and discussion

The principle of LEGs

The experimental device only consists of a commercial TEG module (4 × 4 cm^2, p/n type Bi_2Te_3, Shenzhen Zhiquchuang Technology Co. Ltd) as a generator and pure water, ethanol, or acetone as an evaporation cooling liquid, as shown in Fig. 1a. A multimeter is used to measure the current/voltage during the liquid evaporation. The simplified cross-section TEG module is schematically presented in Fig. 1b, where water at the top layer is used for evaporation cooling and produces a cold surface at the Al_2O_3 insulation layer (the TEG surface layers of both sides). The p-type TE element and n-type TE element at the middle layer are connected by conductive wires in a tandem way. The Al_2O_3 insulation layer is also placed at the bottom layer, which is directly connected to the ambient atmosphere and can serve as a hot side. During the evaporation, heat will spontaneously flow from the bottom Al_2O_3 layer to the upper Al_2O_3 layer (Fig. 1c) due to their temperature differences (ΔT) < 0. The ΔT will form a driving force to drive the carriers in the p/n TE elements to move at the same direction. As a result, evaporation cooling-induced electricity is generated based on the Seebeck effect (Fig. 1d). Fig. 1e and f present the photograph of the cross-section and top-view of the real TE module.

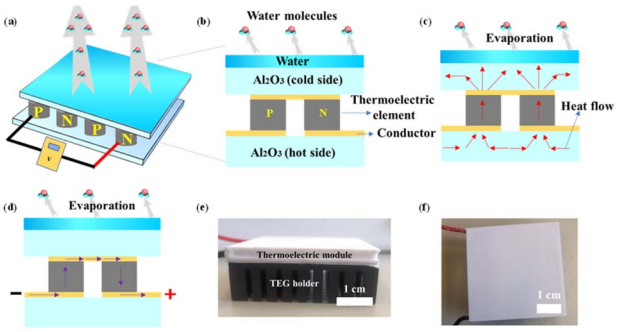

Fig. 1 Structure of LEGs (we take water evaporation as the cold source for the TE). (a) A schematic picture of the w-LEG assembled from large quantities of p- and n-type thermoelectric elements. (b) Illustration of the simplified cross-section of the w-LEG. (c) Illustration of the heat flow direction, and (d) current direction within the w-LEG. Photographs of (e) the side-view and (f) the top-view thermoelectric module.

During evaporation-induced cooling, the electrical power is generated by the thermoelectric device with the resulting temperature difference between the two sides of the TEG device. The bottom side remains at ambient temperature or room temperature, and the temperature of the top side is reduced due to the evaporative cooling. Evaporative cooling actually exploits the energy transfer through evaporation (enthalpy of vaporization). An amount of heat will be absorbed by the liquid from its surroundings in order to evaporate so that the temperature (including the top side of the TEG device) is significantly lower than that of the surroundings (including the bottom side of the TEG device). The temperature difference originates from the phase transition of a liquid to vapor, *i.e.* the latent heat. Usually, larger ΔT leads to more power generation. Generally, the amount of temperature drop by evaporative cooling is dependent on the amount of energy transfer from liquid to vapor, and this means it depends on the enthalpy of vaporization (liquid type) and the evaporation rate. The different performances of the w-LEG, e-LEG, and a-LEG are mainly due to the different enthalpy of vaporization. For the same evaporation rate, a larger enthalpy of vaporization leads to a larger drop of temperature. The evaporation rate, for instance of water, depends on many further factors, such as flow rate of air, temperature, humidity, pressure, area, and so on. In case of a liquid thin film on a substrate, it is more complicated and the wetting or dewetting behaviour and kinetics should be also considered. In this study, we have typically studied the influence of air flow rate.

Liquid evaporation and electricity generation

To confirm the evaporation cooling as the origin of the cold source, the effects of different liquid evaporation cooling are systematically measured using an infrared (IR) camera. The bare TE module is applied as the control experiment and its surface temperature is recorded using an IR camera in real time at room temperature. The results (Fig. 2a) show that the surface

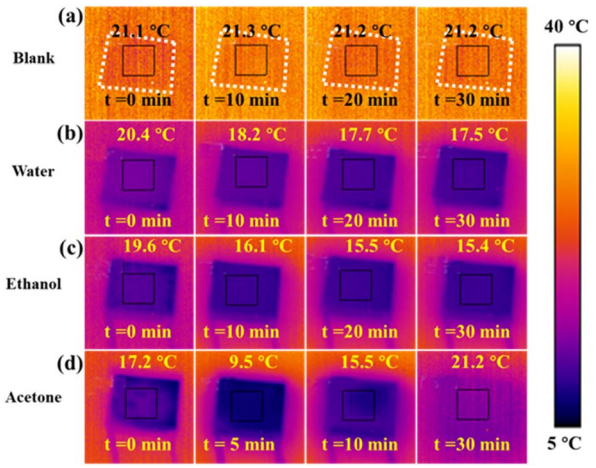

Fig. 2 The temperature changes of the various liquids, which evaporate at the upper TEG junction. (a) The control group remains at room temperature. The dashed box is the TEG device. (b–d) The surface temperature changes with time with free water evaporation, ethanol evaporation, and acetone evaporation, respectively.

temperature of the bare TE module almost remains the same for the whole 30 minutes, while there are remarkable temperature changes in response to evaporation as covered with about 2 mL of water (Fig. 2b), ethanol (Fig. 2c), and acetone (Fig. 2d). It takes 30 minutes for water evaporation and ethanol evaporation to achieve maximum ΔT (between the room temperature and final temperature) of 4.7 and 5.7 °C, respectively, while only 5 minutes are needed to obtain a maximum ΔT of 10.7 °C for acetone evaporation. After 5 min, the covered area of acetone begins to reduce. This is because water, ethanol and acetone have different evaporation rates and different evaporation enthalpies at room temperature,[21–26] and therefore different amounts of absorbed heat from the ambient atmosphere (Fig. S1a–c†). Finally, acetone is totally evaporated out at 7 min and the surface temperature of the TE module returns back to room temperature at 30 min (Fig. 2d). The surface temperature of different TE modules changing with time is presented in Fig. S2a.† Since the bare TE module maintains the thermal equilibrium with the ambient atmosphere, there are almost no detectable current (red line in Fig. S2b†) and voltage (red line in Fig. S2c†), indicating that no current/voltage can be produced. The steady current/voltage produced by water (pink lines in Fig. S2b and c†) and ethanol (blue lines in Fig. S2b and c†) evaporation is due to the stable evaporation rate and thermal coupling between the device and the atmosphere. However, the current and voltage change clearly or at first decrease and then increase for acetone evaporation, because of the fast evaporation (maximal surface temperature change at t = 5 min and total out-evaporation at t = 7 min, as indicated also from the green line in Fig. S2b and c†). After the acetone is totally evaporated out, the current/voltage become ignorable.

W-LEG works in a simulated real environment

Out of safety reasons and cost-effectiveness,[27,28] we use water evaporation-induced electricity as the major research direction. In a practical environment, it is always inevitably accompanied by wind. Therefore, wind velocity-dependent voltage generated by water evaporation and TE module is measured, as shown in Fig. 3a. Obviously, the wind velocity will enlarge the output voltage, because large wind velocity can promote the water evaporation rate and thus lead to a lower surface temperature. As a result, the output voltage is increased with the winds speed. By fitting the voltage data at different wind velocities, the output voltages show a good linear relationship (the linear factor is 0.908) with the wind velocity (Fig. 3b). It verifies that strong wind is beneficial for electric power generation using the w-LEG based on the Seebeck effect. We also try to measure the voltage when the wind is turned on and off.

The data presented in Fig. 3c indicate that the voltage increases from 6.5 mV to 30.3 mV while maintaining a wind speed of 2 m s^{-1}. Conversely, when the wind is ceased, there is a gradual decrease in voltage. Additionally, the voltage continues to increase once the wind is reintroduced, thereby demonstrating that enhanced evaporation due to wind acceleration contributes to an increase in output voltage. The peak value in Fig. 3c shows the maximum ΔT between both sides of the TEG due to continuous evaporation, resulting in the lowest temperature at t = 120 s. While the fan is turned off, the evaporation gradually slows down, and the ΔT also becomes small in the period of 120–180 s.

As a demonstration of the potential application, we explored the performance of the w-LEG at a ΔT (the temperature at the hot side minus the ambient temperature) <25 °C, which widely exists in daily life. The performance of the single w-LEG is measured at a rising ΔT temperature at a wind velocity of 2 m s^{-1}, and the output voltage trend (Fig. 3d) increases as the ΔT increases. When the ΔT arrives at the maximum value of 17.1 °C at five minutes, the output voltage also achieves a maximum value of 0.66 V. To distinguish the contribution of water evaporation, the output voltage of the bare TE module at a wind velocity of 2 m s^{-1} is measured, and its maximum voltage is only 0.13 V and changes frequently due to the loss of water cooling. Thus, water evaporation can clearly improve the output voltage. The short-circuit current at the same wind velocity is also measured. As shown in Fig. 3e, the current also increases with the rising ΔT; the maximum value of current is 130 mA at t = 4 min and the current drops a little due to a tiny temperature fluctuation. Because the voltage of 0.66 V is still not high enough to power the common electronic devices, such as LED lights, cell phones, electronic watches, and so on. We attempt to connect five w-LEGs in series and the output voltage of 5 w-LEGs greatly enhances up to 4.4 V at t = 4 min, and the voltage shows a bit decrease to 3.8 V, exceeding the output voltage of two junctions of a commercial AA battery. However, the five connected TE modules without water evaporation cooling can only produce a maximum output voltage of 0.59 V at t = 2 min because of the fast thermal diffusion from the hot side to the cold side, which demonstrates that water evaporation cooling can be effectively used to enhance the output voltage of the device.

Practicality and scalability of the w-LEG

Fig. 4a shows the schematic illustration of our assembled 5 w-LEGs, where wind generated by a fan is used for accelerating

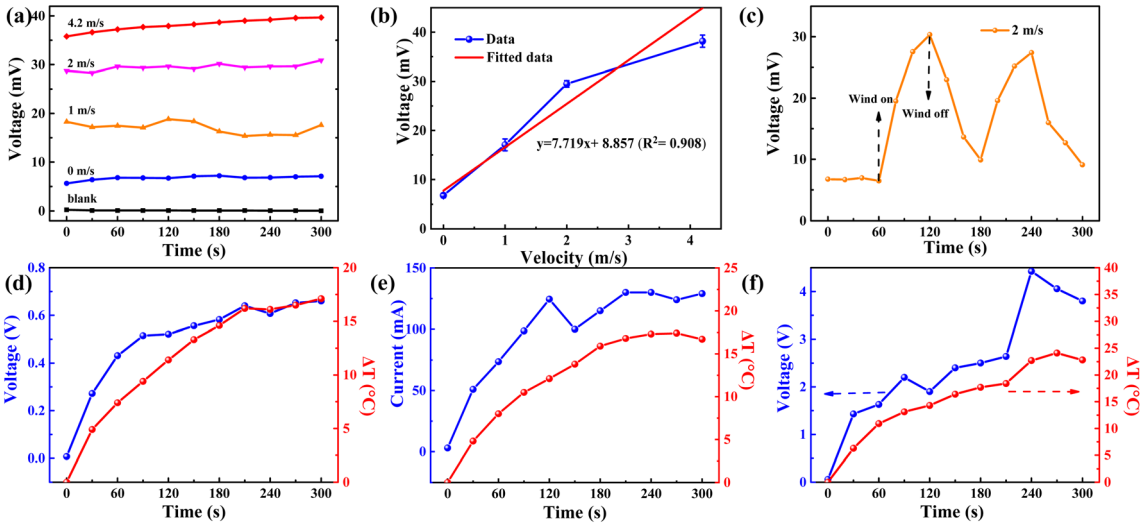

Fig. 3 Performance of single and scalable w-LEGs under practical conditions. (a) Measured open-circuit voltages of the single w-LEG at different wind velocities. (b) The relationship between open-circuit voltage and wind velocity for the single w-LEG. (c) Open-circuit voltage responsive curve with repeatedly wind-on and wind-off. (d) Open-circuit voltage, and (e) short-circuit current of the single w-LEG at a surface with increasing temperature. (f) Open-circuit voltage of five w-LEGs at a surface with increasing temperature.

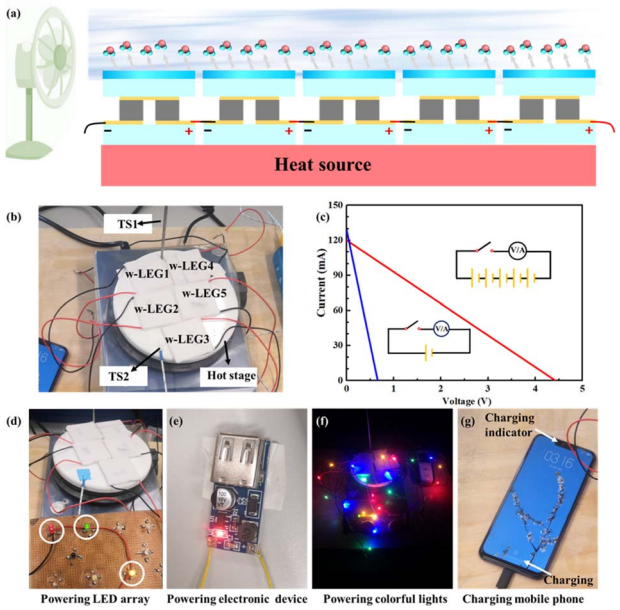

Fig. 4 Electric power generation and applications of electricity produced by w-LEGs. (a) Schematic image of electricity generation of 5 tandem w-LEGs. (b) The photograph of the real device for a. TS1 represents the temperature sensor for the hot stage; TS2 is the temperature sensor for the practical temperature measurements. (c) Voltage–current curves of the single w-LEG (blue) and 5 tandem w-LEGs (red). (d–g) The 5 tandem w-LEGs can supply power for different electronic devices, such as (d) a LED array, (e) a circuit indicator, (f) colorful lights, (g) a cell phone using a 5 V voltage convertor.

water evaporation to maintain the cooling effect, and five tandem TE modules are placed on the hot stage to produce electricity. Fig. 4b is the real device. The single w-LEG (blue line in Fig. 4c) can offer a voltage of 0.66 V and a current of 130 mA, and the 5 tandem w-LEGs (red line in Fig. 4c) can achieve a maximum voltage of 4.4 V and a current of 120 mA at $\Delta T = 22.7$ °C. Surprisingly, they are able to exhibit a maximum power density of 5.4 mW cm^{-2}, surpassing one to six orders of magnitude than state-of-the-art water evaporation-induced electricity devices (Table 1). The corresponding power of 5 tandem w-LEGs is presented in Fig. S5† and the maximum power is 0.43 W when the load resistance (R_L) is equal to the inner resistance (R_{in}). As a result, the 5 tandem w-LEGs can provide large enough voltage/power for common electronic devices, such as three parallel connections of red, green and yellow LED lights (Fig. 4d), an electronic indicator (Fig. 4e), and a string of colorful lights (Fig. 4f and Video S1†). The 5 tandem w-LEGs even can power for mobile phones (Fig. 4f) with the assistance of a voltage amplifier, which can automatically convert the voltage of 5 tandem w-LEGs into 5 V.

Table 1 The performance comparison with the latest water evaporation generators (WEGs)

WEGs	Principle	V	A	Power density	Ref.
CB/MWCNT[a]	HV[g]	4.8 V	100 nA	—	5
Biofilm	HV	2.38 V	~0.8 μA	0.69 mW cm^{-2}	9
Al/Al	HV	3.76 V	1.47 mA	—	29
LS-TENG[b]	HV	1.4 V	0.3 μA	—	10
MOF[c]	HV	0.6 V	—	1.56 nW cm^{-2}	30
CNM[d]	HV	1.105 V	8.57 μA	25.3 μW g^{-1}	31
SiNW[e]	HV	1.75 V	43 μA	6 μW cm^{-2}	8
rGO[f]	HV	2.34 V	44 μA	1.74 μW cm^{-2}	7
ZnO	HV	0.4 V	20 nA	—	32
SiNW	HV	3.7 V	0.3 μA	160 μW cm^{-3}	33
TE module	Seebeck	4.4 V	120 mA	5.4 mW cm^{-2}	Our work

[a] CB/MWCNT: carbon black/multi-wall carbon nanotube. [b] LS-TENG: liquid–solid triboelectric nanogenerator. [c] MOF: metal–organic framework. [d] CNM: carbon nanofiber mat. [e] SiNW: silicon nanowire. [f] rGO: reduced graphene oxide. [g] HV: hydrovoltaic.

Conclusions

In summary, we have demonstrated three types of liquid evaporation generators based on the Seebeck effect, capable of producing maximum short-circuit currents of approximately 24 mA, 6 mA, and 3 mA, along with maximum open-circuit voltages of 55 mV, 14 mV, and 8 mV for the a-LEG, e-LEG, and w-LEG, respectively, at room temperature. To enhance the performance of these generators, specific environmental conditions such as high-temperature atmospheres, low relative humidity levels, efficient heat dissipation systems, and strong airflow are crucial. For instance, a series of five w-LEGs in tandem can generate a voltage of 4.4 V, surpassing the output of two commercial AA batteries and achieve a peak power of 0.43 W at 40 °C with a wind speed of 2 m s^{-1}. This remarkable performance outshines recent water evaporation generators based on the hydrovoltaic principle, highlighting the simplicity and effectiveness of our experimental setup. The practical utility of w-LEGs is evident in applications such as LED lighting and mobile phone charging, showcasing their potential for further advancement and scalable production towards sustainable electricity generation. The major limitations of LEGs are low output voltage and continuous liquid supply. Future research endeavours should concentrate on enhancing water evaporation rates, optimizing thermal management, and improving the figure of merit of thermoelectric generators to facilitate large-scale electricity generation through LEGs. This novel approach presents a user-friendly and environmentally friendly method for electricity generation, offering innovative solutions to address the global energy challenges.

Data availability

The data supporting this article have been included as part of the ESI.†

Author contributions

All authors discussed and wrote this work together.

Conflicts of interest

There are no conflicts to declare.

Acknowledgements

This work was supported by Deutsche Forschungsgemeinschaft (DFG grant Scha 632/24, Tailored Disorder). Björn Müller is acknowledged for offering an IR camera and its calibration. Additionally, Pengfei Cheng is supported by a China Scholarship Council (CSC) fellowship.

Notes and references

1 J.-F. Pekel, A. Cottam, N. Gorelick and A. S. Belward, *Nature*, 2016, **540**, 418–422.
2 G. Zhao, Y. Li, L. Zhou and H. Gao, *Nat. Commun.*, 2022, **13**, 3686.
3 L. Bengtsson, *Environ. Res. Lett.*, 2010, **5**, 025202.
4 T. Oki, D. Entekhabi and T. Harrold, *Washington DC American Geophysical Union Geophysical Monograph Series*, 2004, pp. 225–237.
5 G. Xue, Y. Xu, T. Ding, J. Li, J. Yin, W. Fei, Y. Cao, J. Yu, L. Yuan, L. Gong, J. Chen, S. Deng, J. Zhou and W. Guo, *Nat. Nanotechnol.*, 2017, **12**, 317–321.
6 A. T. Liu, G. Zhang, A. L. Cottrill, Y. Kunai, A. Kaplan, P. Liu, V. B. Koman and M. S. Strano, *Adv. Energy Mater.*, 2018, **8**, 1802212.
7 G. Zhang, Z. Duan, X. Qi, Y. Xu, L. Li, W. Ma, H. Zhang, C. Liu and W. Yao, *Carbon*, 2019, **148**, 1–8.
8 Y. Qin, Y. Wang, X. Sun, Y. Li, H. Xu, Y. Tan, Y. Li, T. Song and B. Sun, *Angew. Chem.*, 2020, **132**, 10706–10712.
9 Q. Hu, Y. Ma, G. Ren, B. Zhang and S. Zhou, *Sci. Adv.*, 2022, **8**, eabm8047.
10 J. Chi, C. Liu, L. Che, D. Li, K. Fan, Q. Li, W. Yang, L. Dong, G. Wang and Z. L. Wang, *Advanced Science*, 2022, **9**, 2201586.
11 S. Fang, J. Li, Y. Xu, C. Shen and W. Guo, *Joule*, 2022, **6**, 690–701.
12 F. J. DiSalvo, *Science*, 1999, **285**, 703–706.
13 A. W. Van Herwaarden and P. M. Sarro, *Sens. Actuators*, 1986, **10**, 321–346.
14 Z.-H. Zheng, X.-L. Shi, D.-W. Ao, W.-D. Liu, M. Li, L.-Z. Kou, Y.-X. Chen, F. Li, M. Wei, G.-X. Liang, P. Fan, G. Q. (Max) Lu and Z.-G. Chen, *Nat. Sustain.*, 2023, **6**, 180–191.
15 M. Scheele, N. Oeschler, K. Meier, A. Kornowski, C. Klinke and H. Weller, *Adv. Funct. Mater.*, 2009, **19**, 3476–3483.
16 L.-D. Zhao, S.-H. Lo, Y. Zhang, H. Sun, G. Tan, C. Uher, C. Wolverton, V. P. Dravid and M. G. Kanatzidis, *Nature*, 2014, **508**, 373–377.
17 Z.-G. Chen, X. Shi, L.-D. Zhao and J. Zou, *Prog. Mater. Sci.*, 2018, **97**, 283–346.
18 N. Van Toan, T. Thi Kim Tuoi, N. Van Hieu and T. Ono, *Energy Convers. Manage.*, 2021, **245**, 114571.
19 D. Gielen, F. Boshell, D. Saygin, M. D. Bazilian, N. Wagner and R. Gorini, *Energy Strategy Rev.*, 2019, **24**, 38–50.
20 R. P. Allan, M. Barlow, M. P. Byrne, A. Cherchi, H. Douville, H. J. Fowler, T. Y. Gan, A. G. Pendergrass, D. Rosenfeld, A. L. S. Swann, L. J. Wilcox and O. Zolina, *Ann. N. Y. Acad. Sci.*, 2020, **1472**, 49–75.
21 J. L. Monteith, *Q. J. R. Meteorol. Soc.*, 1981, **107**, 1–27.
22 B. Henderson-Sellers, *Q. J. R. Meteorol. Soc.*, 1984, **110**, 1186–1190.
23 K. S. Birdi, D. T. Vu and A. Winter, *J. Phys. Chem.*, 1989, **93**, 3702–3703.
24 C. E. Wyman and N. D. Hinman, *Appl. Biochem. Biotechnol.*, 1990, **24–25**, 735–753.
25 K. Aoki, C. Bardos and S. Takata, *J. Stat. Phys.*, 2003, **112**, 629–655.
26 D. Soldatov, É. Ukraintseva and V. Logvinenko, *J. Struct. Chem.*, 2007, **48**, 938–948.
27 S. C. Bondy, *Toxicol. Lett.*, 1992, **63**, 231–241.
28 D. Joshi and N. Adhikari, *J. Pharm. Res. Int.*, 2019, 1–18.
29 T. Tabrizizadeh, Z. She, K. Stamplecoskie and G. Liu, *ACS Omega*, 2022, **7**, 28275–28283.

30 Z. Wang, Y. Wu, K. Xu, L. Jiang, J. Sun, G. Cai, G. Li, B. Y. Xia and H. Liu, *Adv. Funct. Mater.*, 2021, **31**, 2104732.
31 T. Tabrizizadeh, J. Wang, R. Kumar, S. Chaurasia, K. Stamplecoskie and G. Liu, *ACS Appl. Mater. Interfaces*, 2021, **13**, 50900–50910.
32 S. G. Yoon, Y. Yang, J. Yoo, H. Jin, W. H. Lee, J. Park and Y. S. Kim, *ACS Appl. Electron. Mater.*, 2019, **1**, 1746–1751.
33 B. Shao, Y. Wu, Z. Song, H. Yang, X. Chen, Y. Zou, J. Zang, F. Yang, T. Song, Y. Wang, M. Shao and B. Sun, *Nano Energy*, 2022, **94**, 106917.